Anechoic Chamber Performance Characterization Using Spherical Near-Field Imaging Techniques

Carl W. Sirles, John C. Mantovani, A. Ray Howland, Beau J. Hart

The Howland Company, Inc.
4540 Atwater Court, Buford, Georgia, USA
csirles@thehowlandcompany.com
jmantovani@thehowlandcompany.com
rhowland@thehowlandcompany.com
bhart@thehowlandcompany.com

***Abstract*— Characterizing the electromagnetic performance of anechoic chambers, particularly large anechoic chambers, can be complex and time consuming. Two measurement techniques commonly used for chamber characterization include Free Space VSWR and Quiet Zone Probing. The data produced by these chamber evaluation techniques is generally not sufficient to fully characterize the entire chamber. This paper presents a characterization technique utilizing Spherical Near-Field Imaging which provides data sufficient to determine the level and direction of signals reflected from all anechoic chamber surfaces and fixtures which enter the Quiet Zone, and to determine the extraneous signal level within a specified Quiet Zone volume. The basis of the measurement technique is described and typical chamber test results are discussed.**

I. Introduction

Anechoic chambers are intended to simulate a free-space environment within a protected, closed volume. Reflections from chamber surfaces deviate from free-space conditions and introduce errors into electromagnetic measurements made within the chamber. To quantify the measurement error, the chamber must be evaluated to determine the level of extraneous signals present within a defined measurement volume. Comprehensive evaluation of large chambers designed to provide large test volumes and to operate over wide frequency ranges can be complex and time consuming. Two techniques have been widely used to characterize such chambers: Free Space VSWR and Quiet Zone Linear Probing.

Free Space VSWR [1] uses a directive probe antenna to sample the signal level reflected from finite areas of the chamber walls at selected specular reflection angles. A linear field-probe is used to move (scan) the probe antenna along a linear path parallel or perpendicular to the chamber surface to be evaluated with the probe antenna set to the desired specular angle. A scan must be made for each specular reflection angle to be evaluated. And, the field-probe must be re-positioned to cover each chamber surface area to be evaluated. Each scan provides amplitude vs. linear position data which are sufficient to characterize the level of the signals reflected from the chamber surfaces at various specular angles. However, it is generally impractical to evaluate the entire area of each chamber surface.

The Quiet Zone of an anechoic chamber is a defined volume within the chamber where a Device Under Test (DUT) is to be placed for evaluation. Quiet Zone Probing is accomplished by moving a probe antenna through the Quiet Zone to determine the level of extraneous signals entering the volume. Quiet Zone Probing most often uses one-dimensional scanners (field- or phase-probes) or two-dimensional (x-y) scanners. The probe antenna is moved along lines or planes within the Quiet Zone volume. Each scan provides amplitude (and phase) vs. linear position data which is sufficient to characterize the level of extraneous signals in the Quiet Zone at the position of the scan. Angle-of-Arrival of the extraneous signals can also be determined in some cases. While this technique can adequately characterize electromagnetic field purity within the Quiet Zone, it provides very limited information on the performance of any individual surface or fixture of the anechoic chamber.

In contrast to the above techniques, Spherical Near-Field Imaging [2], [3], [4], [5], [6], [7] lends itself to detailed characterization of the chamber surfaces and fixtures as well as determination of electromagnetic field purity within a specified Quiet Zone volume. In Spherical Near-Field Imaging, a probe antenna is scanned over a spherical surface bounding a pre-determined Quiet Zone within the anechoic chamber. The probe antenna is mounted radially and points outward toward the chamber surfaces. The amplitude and phase information recorded at each spherical sample point on the measurement sphere is processed using a Near-Field Imaging algorithm and the resulting signal amplitude data is plotted against angle-of-arrival to provide a graphical representation of the signal components entering the Quiet Zone. The angle-of-arrival of reflections can be used to isolate the source of extraneous signals to specific chamber surfaces or fixtures.

II. Measurement System

The measurement system required for Spherical Near-Field Imaging is conceptually simple, but careful design is required to achieve optimum system performance.

A. The Spherical Scanner

Spherical Near-Field Imaging utilizes a spherical coordinate system whose origin is coincident with the center of a defined spherical Quiet Zone volume as shown in Figure 1. RF data is sampled on a spherical surface of defined

radius r centered on the coordinate system origin. Sampling intervals in both θ and φ directions must satisfy the Nyquist criteria at the measurement radius.

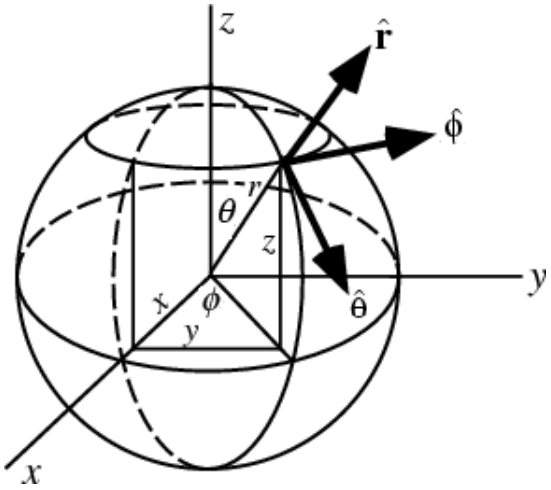

Figure 1. Spherical Near-Field Imaging Coordinate System

A Roll-Over-Azimuth scanner configuration is well-suited for this application. An example of a scanner designed specifically for this type of measurement is shown in Figure 2. Motion in the spherical θ direction is provided by the roll positioner; motion in the spherical φ direction is provided by the azimuth positioner. The roll positioner is mounted on a tower which is offset from the azimuth axis such that the boresight axis of the probe antenna intersects the spherical coordinate origin, thus data is collected along Great Circle cuts of the spherical surface.

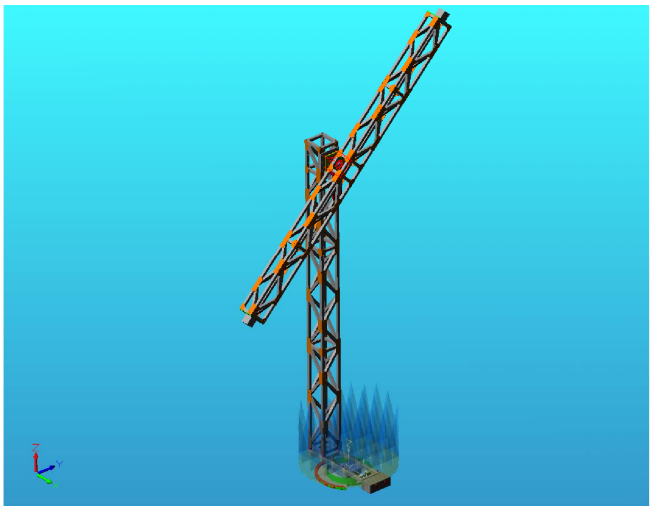

Figure 2. Roll-Over-Azimuth Spherical Scanner

Reflections from the scanner structure will be present in the imaged data. To minimize the level of these signals, the tower and boom elements of the scanner are constructed of low dielectric composite materials. The truss configuration of these elements provides low mass and excellent structural stiffness (compliance).

Alignment of the scanner is extremely important if high resolution images are to be obtained. Axis intersection and perpendicularity should be less than 0.02 wavelengths at the highest desired measurement frequency. Scanner alignment is accomplished through the use of laser fixturing.

Positional accuracy of the scanner is equally important to high resolution imaging. Position accuracy should be less than one tenth of the angular sample interval at the highest desired measurement frequency.

B. The RF System

A Vector Network Analyzer based RF system is used to measure the amplitude and phase of the composite signal entering the probe antenna at each sample point. This configuration is inherently broadband so that wideband measurements can be made by changing only the probe antenna. A simplified block diagram of a typical RF system is shown in Figure 3.

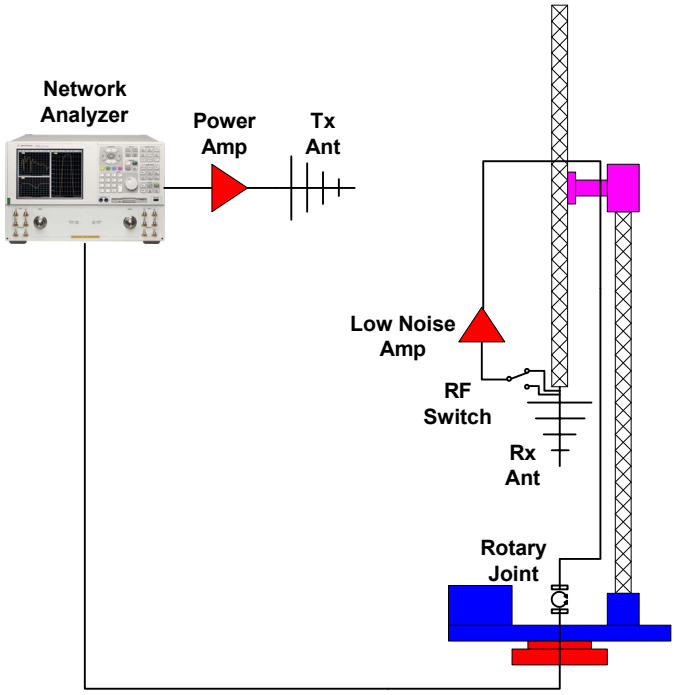

Figure 3. RF Measurement System Block Diagram

Spherical Near-Field imaging requires the measurement of the amplitude and phase of the composite signal entering the probe antenna. Stability of the measurement system is extremely important, particularly during long data acquisition runs. High quality, phase and amplitude stable RF cables should be used throughout the system. Temperature variation within the anechoic chamber should be less than 5 degrees C over the duration of data acquisition.

Measurement system dynamic range is the most important parameter of the RF system. To minimize image degradation due to system noise, receiver sensitivity should be at least 20 dB lower than the desired minimum signal level to be imaged.

C. The Probe Antenna

The probe antenna is possibly the most critical element of the imaging system. For best imaging results, the structure of the probe should confine the radiated energy to the $\mu = \pm 1$ modes [8]. Such probes are typically limited to waveguide bandwidths or less. This complicates the evaluation of chambers over wide bandwidths.

The Front-to-Back (F/B) ratio of the probe assembly is also critical to obtaining high quality images. F/B ratios better than -35 dB are desired. Using an absorber baffle to surround the probe antenna can improve F/B ratio by 10 dB or better.

Several different types of probes have been experimentally evaluated for use with the imaging system. These include rectangular Open Ended Waveguide (OEWG), rectangular waveguide horns, and ridged waveguide horns. A picture of a 4 GHz horn antenna assembly is shown in Figure 4. The absorber shroud has been removed from the mounting plate for clarity.

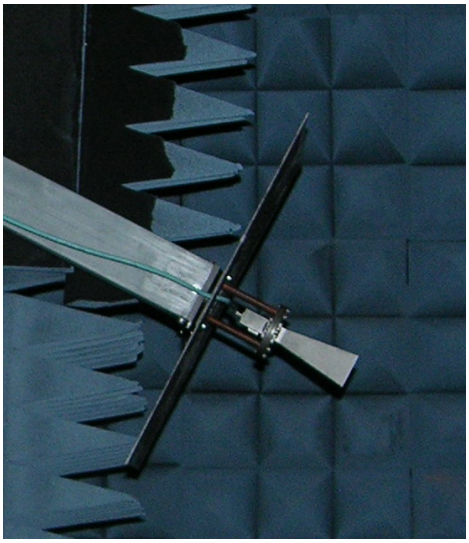

Figure 4. Spherical Probe Antenna Assembly

In general, the simpler antenna structures have higher modal purity and produce better images. The structural complexity of broadband antennas such as ridged waveguide horns generally stimulate higher order modes and degrade image quality.

III. Measurement Software

A. Scanner Control and Data Collection Software

Near-Field Imaging requires the acquisition of amplitude/phase data at equally spaced angular positions around a sphere. For large Quiet Zones and/or high measurement frequencies the number of data samples will exceed 10^6. A LabView® based software suite (Howland WTL software) was used to control the scanner and RF equipment and automatically record the measurement data. The software allows user setup of data acquisition parameters via a Graphical User Interface (GUI), automatically reads and records multi-frequency RF data, and monitors the scanner for fault conditions. Measurement data is stored in ASCII formatted data files for simple importation into the data processing software.

B. Data Transformation and Analysis Software

The raw data recorded at each sample point on the spherical measurement surface is a vector sum of all of the plane waves entering the probe antenna at that sample position. Very little useful information can be generated from this raw data. The data must be processed using a Spherical Near-Field to Far-Field transformation in order to separate the various spatial components of the composite signal.

The US National Institute of Standards and Technology (NIST) in Boulder, Colorado has been involved in Spherical Near-Field techniques and applications for many years [2], [5], [6], [7], [8] and has developed an effective software package for Spherical Near-Field Imaging. This software suite was used as the basis for the data processing software required to evaluate extraneous reflected signals in an anechoic chamber.

The NIST software has been applied to chamber evaluation and chamber imaging [6], [7]. For chamber evaluation the desired information is the magnitude and angle-of-arrival of extraneous reflections which enter the Quiet Zone. A measure of signal purity inside the quiet Zone is also required.

For this application, the NIST software was modified to produce a graphical representation of the angular spectrum of extraneous signals entering the Quiet Zone. The level of an extraneous signal and the respective angle-of-arrival are plotted and can be used to isolate the chamber feature which produced the extraneous signal.

The software was also modified to produce plots of the composite vector signal level within the Quiet Zone along specified linear cuts through the Quiet Zone. This data is identical to the data which would be obtained by Quiet Zone field probing and provides evaluation of amplitude/phase taper and ripple within the Quiet Zone.

IV. Measurement Results

The effectiveness of this anechoic chamber characterization technique has been demonstrated by measurements made in two different anechoic chambers. One chamber is of small size (20ftW x 20ftH x 40ftL) and is intended for antenna measurements at frequencies above 1 GHz. Another chamber is very large (70ftW x 40ftH x 110ftL) and is intended for antenna and EMC measurements at frequencies above 100 MHz.

Angular spectrum data is presented for each chamber at several test frequencies. The data presented is the magnitude of the extraneous signals passing through the spherical Quiet Zone surface as a function of the spherical coordinates (θ,φ). The spherical coordinates are plotted on a rectangular grid for simplicity, thus the spherical surface appears unfolded and flattened. The angular unit is degrees. The $\theta = 0$ direction is looking up toward the chamber ceiling, and the chamber source antenna is located at $(\theta,\varphi) = (90,0)$. The backwall of the chamber is located roughly from $\theta = 230$ to 310 and $\varphi =$

-25 to 25. Amplitude data is referenced to the source antenna level at (θ,φ) = (90,0).

A. Small Chamber Test Results

Figures 5 and 6 show angular spectrum data for the small chamber at 4 and 10 GHz. The background level is -55 dB.

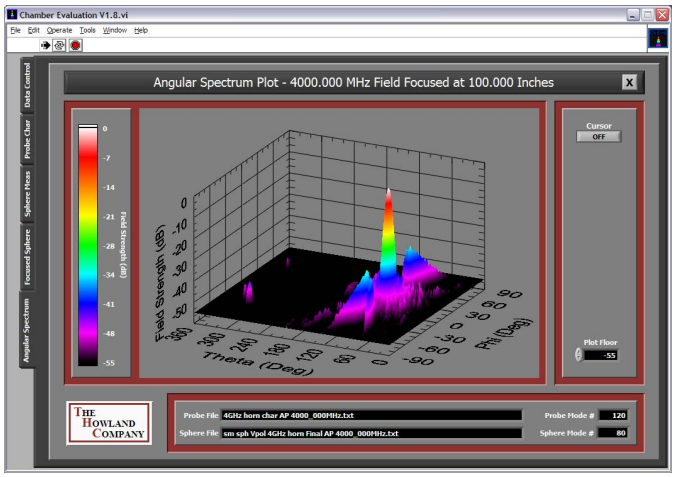

Figure 5. Angular Spectrum for Small Chamber at 4 GHz.

Figure 5 shows three readily identifiable reflections at approximately θ = 325 deg. These reflections are from a camera located high on the chamber sidewall and from two sprinkler pendants located on the ceiling. The reflection levels are -45 to -50 dB.

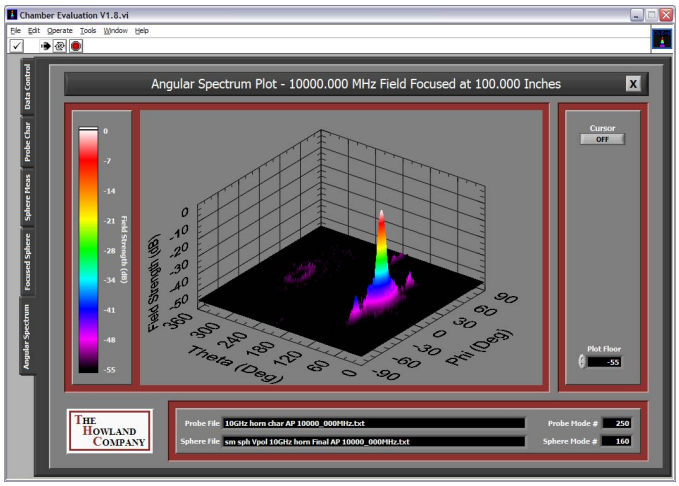

Figure 6. Angular Spectrum for Small Chamber at 10 GHz.

Figure 6 shows reflection patterns at (θ,φ) = (270,0). This location is the center of the chamber backwall. The reflection levels are approximately -50 dB.

Figure 5 shows a pronounced "X" pattern surrounding the main lobe of the source antenna. The cause of this anomaly is being investigated, but is probably not a chamber reflection. It is suspected that excessive energy in modes higher than μ = ±1 in the probe antenna may be causing this effect. The effect is also present in Figure 6, although the geometric "X" pattern is not as obvious. Rectangular horns were used for the probe antenna in both cases.

B. Large Chamber Test Results

Figures 7 and 8 show angular spectrum data for the large chamber at 1 and 4 GHz. The background level is -45 dB at 1 GHz and -70 dB at 4 GHz.

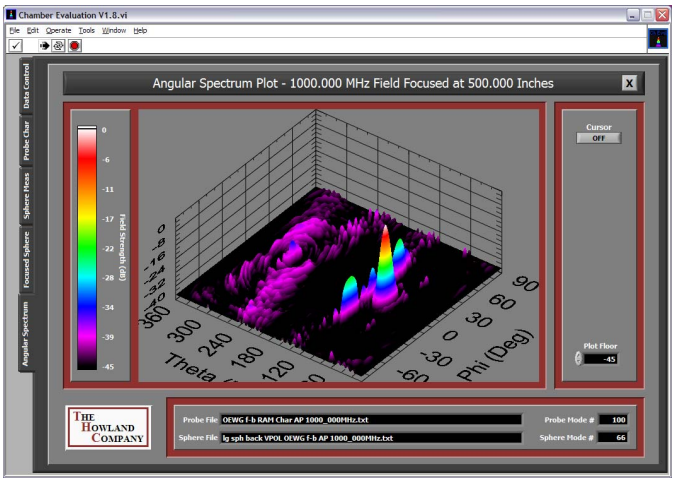

Figure 7. Angular Spectrum for Large Chamber at 1 GHz.

Figure 7 shows broad area reflections from the backwall of the chamber at a level of approximately -40 dB. Also identifiable are specular reflections at (θ,φ) = (120, ±30). These reflections were generated by a row of walkway absorber along each chamber wall.

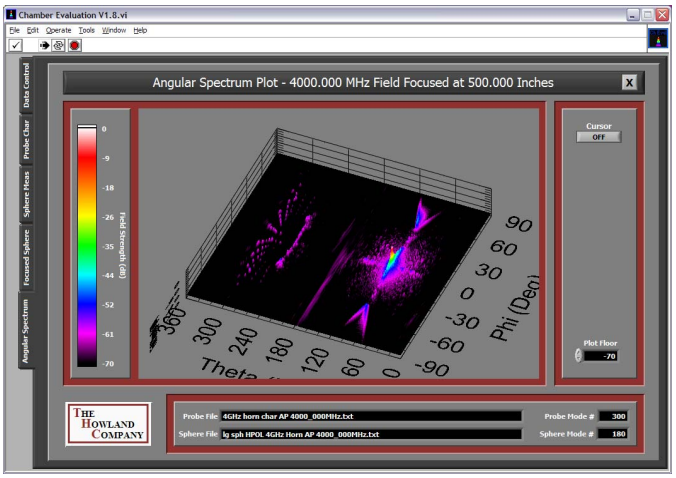

Figure 8. Angular Spectrum for Large Chamber at 4 GHz.

Figure 8 shows a distinct geometric pattern of reflections coming from the rear surfaces of the chamber at a level of approximately -60 dB. These reflections were produced by an array of sprinkler heads located on the walls and ceiling and protruding through the absorber.

The "X" pattern is also present in this figure, although the level of the pattern is less than -50 dB.

V. CONCLUSIONS

An anechoic chamber characterization technique based on Spherical Near-Field Imaging has been presented. A measurement system concept has been described and implemented. Software for measurement system control and data processing has been described. Test results from two different anechoic chambers have been presented.

The test results clearly indicate that extraneous signals as low as -70 dB below the level of the chamber source antenna can be seen. Further, the angle-of-arrival of all energy entering the Quiet Zone can be determined as well as the relative level of all extraneous signals. From this three-dimensional information the features or fixtures of the anechoic chamber that are producing the extraneous signals can be isolated and possibly eliminated.

ACKNOWLEDGMENT

The authors wish to express sincere appreciation for the assistance and support of Dr. Ed Joy, Ron Wittmann, Mike Francis and Randy Direen of NIST, and Dan Williams and Eric Boschert of ARL during the course of this project.

And the measurement results presented in this paper would not have been achieved without the sacrifice and dedicated long term effort of Jim Howland during the data acquisition process.

REFERENCES

[1] F.P. Brownell, "Radio Frequency Anechoic Chambers," *Rantec Microwave Antenna Measurements Short Course*, sec. 3.1.2, July 21-25, 1986.

[2] R.C. Wittmann, "Spherical near-field scanning: Determining the incident field near a rotatable probe," *1990 IEEE Antennas and Propagation Symposium Digest*, pp. 224-227, May 7-11, 1990.

[3] D.N. Black, E.B. Joy, M.G. Guler, R.E. Wilson, and G. Edgar, "Spherical probing of spherical ranges," *Proc. AMTA*, Philadelphia, pp. 14-19 - 14-23, Oct. 8-11, 1990.

[4] D.N. Black, E.B. Joy, J.W. Epple, M.G. Guler, and R.E. Wilson, "The effects of spherical measurement surface size on the accuracy of test zone field predictions," *Proc. AMTA*, Dallas, pp. 239-243, Oct. 4-8, 1993.

[5] R.C. Wittmann, and D.N. Black, "Antenna/ RCS range evaluation using a spherical synthetic aperture radar," *Proc. AMTA*, Seattle, pp. 406-410, Sept. 30 - Oct. 3, 1996.

[6] R.C. Wittmann, and M.H. Francis, "Antenna Range Imaging," *Proc. AMTA*, Philadelphia, pp. 234-236, Oct. 16-20, 2000.

[7] R.C. Wittmann, and M.H. Francis, "Test-Chamber Imaging Using Spherical Near-Field Scanning," *Proc. AMTA*, Denver, pp. 87-91, Oct. 21-26, 2001.

[8] M.H. Francis, and R.C. Wittmann, "Uncertainty Analysis for Spherical Near-Field Measurements," *Proc. AMTA*, Irvine, pp. 43-45, Oct. 19-24, 2003.